

Analyst

Accepted Manuscript



This is an *Accepted Manuscript*, which has been through the Royal Society of Chemistry peer review process and has been accepted for publication.

Accepted Manuscripts are published online shortly after acceptance, before technical editing, formatting and proof reading. Using this free service, authors can make their results available to the community, in citable form, before we publish the edited article. We will replace this *Accepted Manuscript* with the edited and formatted *Advance Article* as soon as it is available.

You can find more information about *Accepted Manuscripts* in the [Information for Authors](#).

Please note that technical editing may introduce minor changes to the text and/or graphics, which may alter content. The journal's standard [Terms & Conditions](#) and the [Ethical guidelines](#) still apply. In no event shall the Royal Society of Chemistry be held responsible for any errors or omissions in this *Accepted Manuscript* or any consequences arising from the use of any information it contains.

Preparation of a poly (3'-azido-3'-deoxythymidine-co-propargyl methacrylate-co-pentaerythritol triacrylate) monolithic column by *in situ* polymerization and click reaction for capillary liquid chromatography of small molecules and proteins[†]

Zian Lin,^{a,b,*} Ruifang Yu,^a Wenli Hu,^a Jiangnan Zheng,^a Ping Tong,^a Hongzhi Zhao,^b and Zongwei Cai,^{b,*}

Received (in XXX, XXX) Xth XXXXXXXXX 200X, Accepted Xth XXXXXXXXX 200X

First published on the web Xth XXXXXXXXX 200X

DOI: 10.1039/b000000x

Combining free radical polymerization with click chemistry via copper-mediated azide/alkyne cycloaddition (CuAAC) reaction in “one-pot” process, a facile approach was developed for preparation of poly (3'-azido-3'-deoxythymidine-co-propargyl methacrylate-co-pentaerythritol triacrylate) (AZT-co-PMA-co-PETA) monolithic column. The resultant poly (AZT-co-PMA-co-PETA) monolith showed a relatively homogeneous monolithic structure, good permeability and mechanical stability. Different ratios of monomers and porogens were used for optimizing the properties of monolithic column. A series of alkylbenzenes, amides, anilines, and benzoic acids were used to evaluate the chromatographic properties of the polymer monolith in terms of hydrophobic, hydrophilic and cation-exchange interactions, and the results showed the poly (AZT-co-PMA-co-PETA) monolith exhibited more flexible adjustment in chromatographic selectivity than that of the parent poly (PMA-co-PETA) and AZT-modified poly (PMA-co-PETA) monoliths. Column efficiencies for toluene, DMF, and formamide with 35,000-48,000 theoretical plates/m could be obtained at a linear velocity of 0.17 mm/s. The run-to-run, column-to-column, and batch-to-batch repeatabilities of the retention factors were less than 4.2%. In addition, the proposed monolith was also applied to efficient separation of sulfonamides, nucleobases and nucleosides, anesthetics and proteins for demonstrating its potential.

1. Introduction

Over the past decades, polymeric monoliths have gained greater acceptance as an alternative to conventional microparticle-packed columns due to the advantages of low back pressure, fast mass transfer rate, and ease of preparation.¹⁻³ Although some purely polymeric monoliths are excellent separation media, further functionalization is of utmost importance in most situations in order to gain the desired chromatographic properties. For example, epoxy groups of the

glycidylmethacrylate (GMA)-based monoliths are typically modified using standard electrophile-nucleophile displacement chemistry, or via ring-opening of a pendant reactive moiety to prepare a wide range of polymer monoliths with a variety of separation modes.⁴⁻⁶ Compared with the single-step copolymerization, postpolymerization functionalization allows independent optimization of porous properties of the generic monolith and surface chemistry. However, the preparation procedure is rather tedious and time-consuming. Moreover, the postpolymerization functionalization sometimes has poor selectivity and efficiency, which may have a negative impact on retention characteristics and separation mechanism.⁷ Therefore, exploring a robust, reliable and high-selectivity immobilization method for preparation of functionalized polymeric monoliths is becoming an urgent topic.

Since its first introduction by Sharpless in 2001,⁸ click reactions including Cu (I)-catalyzed 1,3-dipolar azide-alkyne cycloaddition reaction (CuAAC) and “thiol-ene” reaction, have been widely used in polymer and dendrimer synthesis, bioconjugation and surface modification.⁹⁻¹² Thiol-ene reaction has been attracting great interest since it possesses several advantages such as simplicity, high chemoselectivity and high conversion under mild conditions and has been widely employed for the preparation of polymer-based monoliths and organic-inorganic hybrid monoliths.¹³⁻¹⁵ As an alternative, CuAAC has been established as one of the most reliable approaches for covalent assembly of various molecules.¹⁶⁻¹⁹ This immobilization concept offers several advantages over established immobilization protocols, including mild coupling conditions, excellent coupling yields (higher yields compared to thiol-ene reaction), convenient control of the ligand loading level, and full compatibility with a broad range of functional groups.²⁰ CuAAC is a powerful tool for introduction of various functional molecules onto stationary phases to prepare different packed chromatographic columns or enzymatic reactors.²¹⁻²⁵ It is also worth noting that the adoption of CuAAC immobilization strategy for the preparation of monolithic columns is a recent achievement.²⁶⁻³⁰ Guerrouache et al.²⁶ first reported an application of CuAAC click reaction in the functionalization of macroporous organic polymer monolith. In their work, the monolith based on the copolymerization of nacrlyoxysuccinimide (NAS) and ethylene dimethacrylate (EDMA) was prepared firstly, and then a two-step modification was carried out to graft β -cyclodextrin (β -CD) onto the monolith for chiral capillary chromatography. Similar works were reported by Guo et al.²⁷ and Sun et al.,^{28,29} in which a conventional two-step click modification was adopted for the preparation of silica and polymer monoliths, respectively. More recently, Wu et al.³⁰ developed a facile “one-pot” approach for fabrication of clickable organic-silica hybrid monoliths, where

a) Ministry of Education Key Laboratory of Analysis and Detection for Food Safety, Fujian Provincial Key Laboratory of Analysis and Detection Technology for Food Safety, College of Chemistry, Fuzhou University, Fuzhou, Fujian, 350116, China

b) Partner State Key Laboratory of Environmental and Biological Analysis, Department of Chemistry, Hong Kong Baptist University, 224 Waterloo Road, Kowloon Tong, Hong Kong, SAR, P. R. China
Fax: +86-591-22866135 E-mail: zianlin@fzu.edu.cn (Z.A. Lin); zwc@hkbu.edu.hk (Z.W. Cai)

[†] Electronic Supplementary Information (ESI) available: Experimental details and additional figures. See DOI: 10.1039/c0xx00000x

two clickable monomers with either azido or alkynyl moieties were adopted and the resulting hybrid monoliths were further used for the fabrication of monolith-based enzyme reactors via post-polymerization modification employing CuAAC click reaction. However, the aforementioned approaches were based on two-step or multi-step post modifications, which suffered from longer preparation time and more complicated procedures. Despite this attractive feature of CuAAC click chemistry, there are only a few studies²⁶⁻³⁰ to date on the preparation of monolithic columns using CuAAC strategy and no papers on one-pot preparation of polymeric monoliths by *in situ* free radical polymerization combined with CuAAC click reaction have been reported so far.

3'-azido-3'-deoxythymidine (AZT), as an antiretroviral drug used for the treatment of HIV/AIDS infectiousness, belongs to the family of nucleoside analogues.^{31,32} Owing to its unique chemical structure containing hydrophilic/ionizable nucleoside group and azido group, AZT is regarded as an ideal functional monomer to make polymer monoliths for mixed-mode chromatography. Despite this attractive feature of nucleoside monomers, there are not any papers on this kind of the polymer monoliths and even no papers on the preparation of AZT-based polymer monolithic columns and their applications in separation science have been reported so far.

In this work, we report a facile approach for preparation of poly (AZT-co-propargyl methacrylate-co-pentaerythritol triacrylate) (AZT-co-PMA-co-PETA) monolithic column by combination of free radical polymerization and azide-alkyne cycloaddition "click" reaction in one-pot process, where the vinyl/alkyne-organic monomers and initiator azobisisobutyronitrile (AIBN) were mixed with azido-organic monomer in the presence of copper (I) catalyst. The resulting homogeneous mixture was introduced into a fused capillary for the subsequent click reaction and polymerization to form the polymer monolithic column. With the use of this strategy, polymer monolith with a mixed mode involving hydrophilic/hydrophobic/ion-exchange interactions was successfully prepared. Compared to the conventional post-modification method, this proposed synthesis strategy provides an alternative to prepare diverse polymer monoliths by using a variety of azido/alkyne-organic monomers.

2. Experimental

2.1. Materials

Propargyl methacrylate (PMA) and pentaerythritol triacrylate (PETA) were purchased from Alfa Aesar (Ward Hill, MA, USA). AZT was obtained from J&K Scientific Ltd (Beijing, China). 6-Bromohexanoic acid, copper iodide (CuI) and sulfonamide antibiotics were the products of Aladdin (Shanghai, China). AIBN was obtained from Tianjin Chemistry Reagent Factory (Tianjin, China) and recrystallized with methanol (MeOH) prior to use. Alkylbenzenes, thiourea, anilines, amides, benzoic acids and HPLC-grade acetonitrile (ACN) were obtained from Sinopharm Chemical Reagent (Shanghai, China). Horseradish peroxidase (HRP), myoglobin (Mb), cytochrome C (Cyt C), bovine hemoglobin (Hb) and transferrin (Trf) were purchased from Beijing Dingguo Co. Ltd (Beijing, China). Adenine, thymine, 6-methylaminopurine and 2-deoxyadenosine were obtained from Sigma (St. Louis, MO, USA). Anesthetics were the products of national institute for the control of pharmaceutical and biological products (Beijing, China). All other chemicals were of analytical grade or better. Deionized water was prepared with a Milli-Q water purification system (Millipore, Milford, MA). Capillaries with 370 μm o.d. \times 100 μm

i.d. were the products of Yongnian Optic Fiber Plant (Hebei, China).

2.2. Apparatus

An HPLC pump (Elite P200, Dalian, China) was used for washing the polymeric monolithic columns and testing the backpressure after equilibration of them. All capillary liquid chromatography (cLC) were performed on a TriSep-2100 pressurized capillary electrochromatography (pCEC) system (Unimicro Technologies, Pleasanton, CA, USA). A flow rate of 0.02 mL/min and the UV absorbance of 214 nm were used unless otherwise stated. Samples were injected through an injection valve with an internal 2 μL sample loop. A four-port splitter was set between the injection valve and the monolithic column to split the flow into a desirable and stable flow rate (the actual flow rate after splitting was \sim 80 nL/min). Since the splitting ratio was set at 250:1, the actual injection volume was about 8 nL. The morphology of the polymer monoliths was characterized by a PhilipsXL30E Scanning Electron Microscope (SEM) (Amsterdam, Netherlands). The pore properties of the polymer monolith were measured by using physisorption analyzer (Micromeritics ASAP 2010 porosimeter, USA) at -196 $^{\circ}\text{C}$. Prior to the measurements the monolithic polymers were ground and degassed at 120 $^{\circ}\text{C}$ to a residual pressure lower than 10^{-2} Pa. Fourier transform infrared (FT-IR) spectra of the monolithic columns were recorded using the AVATAR 360 FT-IR spectrophotometer (Nicolet, Waltham, MA, USA), where 3 mg powder sample was mixed with 100 mg KBr.

2.3. "One-pot" preparation of poly (AZT-co-PMA-co-PETA) monolithic column via CuAAC click reaction

In order to covalently anchor the polymer to the capillary wall, the capillary was pretreated with a vinyl silanizing agent according to a method reported previously.³³

For the fabrication of the poly (AZT-co-PMA-co-PETA) monolithic column, the prepolymerization mixture is prepared by dissolving various amounts of AIBN (1.0%, w/w, of monomers and crosslinker), AZT (50~66.5 mg), PMA (27~41 μL), PETA (50~70 mg), and catalyst CuI (0.2 mg) in a binary porogenic solvent, which consisted of DMSO (143~207 μL) and 1-dodecanol (149~235 μL) (Table 1). The mixture was sonicated for 20 min to obtain a homogeneous solution, and then purged with nitrogen for 10 min. Subsequently, the mixture solution was filled into the pretreated capillary (50 cm) to a total length of 25 cm. The capillary was sealed at both ends with rubber stoppers and submerged into water bath at 75 $^{\circ}\text{C}$ for 24 h. After polymerization, the monolithic column was connected to HPLC pump and orderly washed with methanol, 20 mM disodium EDTA and water to remove the porogenic solvents, unreacted reagents and catalyst (Here disodium EDTA was used as eluting solvent to coordinate Cu ion and the coordination compound in the eluate was detected at the wavelength of 760 nm by UV/Vis spectrophotometer.²⁸) As a control, the poly (PMA-co-PETA) monolithic column was also prepared in the absence of AZT and CuI according to the same preparation procedure as described above.

2.4. Preparation of AZT-modified poly (PMA-co-PETA) monolith via a two-step post click modification

For comparison, AZT-functionalized poly (PMA-co-PETA) monolith was also prepared by post modification based on CuAAC click reaction. Briefly, monomer PMA (31 μL) and crosslinker PETA (60 mg) and initiator AIBN (1.5 mg) were

dissolved in a mixture of DMSO (175 μ L) and 1-dodecanol (192 μ L). The mixture was surged ultrasonically and purged with N_2 for 10 min, and then filled into the pretreated capillary (50 cm) to a total length of 25 cm. The capillary was sealed at both ends with rubber stoppers and submerged into water bath at 75 $^{\circ}$ C for 12 h. After the polymerization, the column was connected to an HPLC pump and washed exhaustively with methanol to remove the porogenic solvents and unreacted monomers. For the click reaction step, a solution of AZT (1.5 g) and CuI (40 mg) in 50 mL ACN was continuously pumped through the columns for 24 h at 30 $^{\circ}$ C. The resulting monolithic column was obtained after washing by ACN, 20 mM disodium EDTA and water.

2.5. Calculations

Column permeability (K) reflects through-pore size and external porosity, or a domain size at a constant through-pore size/skeleton size ratio. The permeability of the column was calculated using Darcy's equation:

$$K = F \times \eta \times L / \Delta P \times \pi \times r^2 \quad (1)$$

Where F , η , L , ΔP , and r stand for volume flow rate of the mobile phase, dynamic viscosity of the mobile phase, the column length, the column backpressure, and the inner radius of the column, respectively.³⁴ In this work, MeOH was used as mobile phase and its corresponding value of dynamic viscosity was 0.580 $\times 10^{-3}$ kg/(m \times s) at 25 $^{\circ}$ C.³⁵

The retention factor (k) for the analytes was obtained according to the equation, $k = (t_R - t_0)/t_0$, where t_R is the retention time of the analytes, and t_0 is the retention time of void marker, respectively.

2.6. cLC procedures

The monolithic column was placed in the instrument and equilibrated with the mobile phase until a stable baseline was obtained. Isocratic elution of a series of small molecules was performed to evaluate the retention behaviors of the polymer monolithic column in terms of hydrophobic, hydrophilic, and ion-exchange interactions. Different ratio of ACN/H₂O with or without different pH and concentration of phosphate buffer (PB) were used unless otherwise stated (PB with desired pH was adjusted with HCl or NaOH). Proteins were separated in a linear gradient elution mode. Urine sample was collected from a healthy volunteer, and then diluted 20 times with deionized water, then a known concentration of nucleosides and nucleobases was added to prepare the spiked urine sample.

3. Results and discussion

3.1. Preparation and characterization of poly (AZT-co-PMA-co-PETA) monolithic column

The general scheme for "one-pot" preparation of the poly (AZT-co-PMA-co-PETA) monolithic column based on *in situ* free radical polymerization combined with CuAAC click reaction was illustrated in Fig.1, which involved two major reactions: On the one hand, the free radical polymerization of alkyne-containing monomer (PMA) and crosslinker (PETA) to the formation of the poly (PMA-co-PETA) monolithic skeleton; On the other hand, the CuAAC click reaction between azido-containing AZT and alkyne-containing monolithic skeleton to the formation of the poly (AZT-co-PMA-co-PETA) monolith. Since the composition of the reaction mixture has a great influence on the morphology, permeability and selectivity of the polymer monolith. Several parameters such as the mass ratio of monomer/crosslinker, the amount of AZT, the choice of

porogens, and polymerization temperature were further optimized as shown in Table 1.

Like the synthesis of other types of polymer monoliths, reaction temperature is a critical factor for the synthesis of the poly (AZT-co-PMA-co-PETA) monolithic column. Although CuAAC click reaction can be run at room temperature, it should take several days.²⁵ Meanwhile, free radical polymerization triggered by AIBN is intensively performed at 60~75 $^{\circ}$ C. As a result, different reaction temperatures (60 $^{\circ}$ C, 65 $^{\circ}$ C and 75 $^{\circ}$ C) were investigated and the result showed that homogenous and dense monolith was not formed as the reaction temperature was below 75 $^{\circ}$ C.

The type of porogenic solvent plays a vital role in the preparation of polymer monolith. Herein, a binary porogenic solvent was preferred considering the hydrophobicity of PMA, as well as the solubility of AZT, PETA and CuI. Several porogenic solvents, such as 1-dodecanol/cyclohexanol, diethylene glycol/1,4-butanediol, DMF/ethyleneglycol, and DMSO/1-dodecanol, have been studied in detail. Of these, it was determined that a binary porogen of DMSO/1-dodecanol is best fit for the preparation of the porous poly (AZT-co-PMA-co-PETA) monoliths. In this work, the ratio of monomers to porogens was fixed at 30:70 (Table 1). It was observed that with an increase in weight percentage of 1-dodecanol to total porogens from 24.5% to 38.5% (Column E, C and F in Table 1), the back pressure of the polymer monoliths dramatically decreased from 35 MPa down to 12.1 MPa at a linear flow rate of 10.61 mm/s, suggesting that 1-dodecanol acts as a macroporogenic solvent to provide good bulk flow properties.³⁶ Accordingly, DMSO decreased from 45.5% to 31.5% not only dissolved AZT, PETA and CuI well, but also favored the formation of micropores.³⁷ Although the low back pressure of column F was acceptable, the polymer monolith showed low column efficiency and poor resolution (Data not shown). Therefore, DMSO/1-dodecanol with the mass ratio of 38.5/31.5 (wt %) was chosen as the optimum porogens for further studies.



Fig.1. Scheme for one-pot synthesis of the poly (AZT-co-PMA-co-PETA) monolithic column based on *in situ* free radical polymerization combined with CuAAC click reaction.

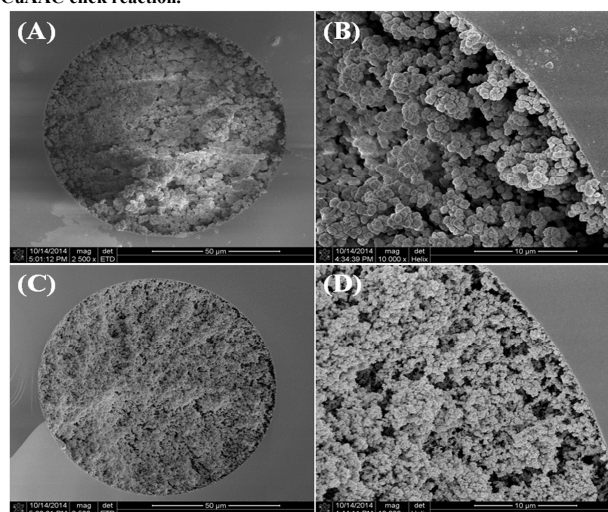


Fig.2. SEM images of poly (PMA-co-PETA) monolith: (A) $\times 2500$ and (B) $\times 10000$. Poly (AZT-co-PMA-co-PETA) monolith: (C) $\times 2500$ and (D) $\times 10000$.

Table 1. Effects of synthesis parameters on the formation of poly(AZT-co-PMA-co-PETA) monolith*

Columns**	Monomers			Porogens		Crosslinker	Backpressure (MPa)*	Permeability ($\times 10^{-14} \text{ m}^2$)
	AZT (wt %)	PMA (wt %)	Molar ratio of AZT/PMA	DMSO (wt %)	1-Dodecanol (wt %)	PETA (wt %)		
A ^a	10.0	8.0	0.6	38.5	31.5	12.0	17.5	8.89
B ^a	10.7	5.3	1.0	38.5	31.5	14.0	26.5	5.87
C ^{a,b}	12.0	6.0	1.0	38.5	31.5	12.0	27.6	5.64
D ^a	13.3	6.7	1.0	38.5	31.5	10.0	28.4	5.48
E ^b	12.0	6.0	1.0	42.5	24.5	12.0	Too high to pump	--
F ^b	12.0	6.0	1.0	31.5	38.5	12.0	12.1	12.86
G ^c	0	6.0	--	38.5	31.5	12.0	12.0	12.80

* Flushed with MeOH; Flow rate, 5 $\mu\text{L}/\text{min}$ (Linear flow rate: 10.61 mm/s); ** (a) the effect of the ratio of monomer/crosslinker; (b) the effect of porogens; (c) the control monolith

The ratio of monomer to crosslinker affects not only the rigidity and permeability, but also the chromatographic selectivity and column efficiency. Since the CuAAC click reaction proceeded with chemoselectivity and equimolarity, thus the molar ratio of AZT to PMA was better kept equimolar. To investigate the influence of the mass ratio of total monomer (AZT and PMA) to crosslinker (PETA), four monoliths (Column A–D, Table 1) were prepared by varying total monomer weight percentages from 16% to 20%, in which the weight percentage of PETA accordingly changed from 14% to 10%. Using different solvents (MeOH and water), a linear dependence of flow rate on column back pressure was observed in a series of columns (Fig.S1, Supporting information), indicating these monoliths have good mechanical stability. Furthermore, an increase in monomers or decrease in crosslinker, back pressure of the monoliths gradually increased and the corresponding permeabilities decreased as listed in Table 1. It was suggested that high ratio of monomer to crosslinker favored the formation and aggregation of smaller microglobules inside the capillary during copolymerization process, and thus resulted in high back pressure.

Fig.2(A-D) showed the SEM images of the poly (PMA-co-PETA) monoliths incorporated with and without AZT via CuAAC click reaction. Overall, these monoliths showed a uniform monolithic structure with good attachment to the inner wall of the capillary. Compared to the poly (PMA-co-PETA) (Fig.2(A-B)) monolith, however, a full dense and homogeneous monolithic skeleton with smaller microglobules was observed in the poly (AZT-co-PMA-co-PETA) monolith (Fig.2(C-D)), suggesting the successful immobilization of AZT via click reaction in “one-pot” process. In addition, the pore properties of the polymer monoliths were also characterized by nitrogen adsorption-desorption measurement. The specific surface area and average pore diameter of the poly (AZT-co-PMA-co-PETA) monolith were calculated to be 178.4 m^2/g and 7.35 nm, much better than those of the poly (PMA-co-PETA) monolith, where the corresponding values were 26.6 m^2/g and 16.8 nm, respectively.

FT-IR spectra provide a direct proof of “one-pot” synthesis of the poly (AZT-co-PMA-co-PETA) monolith, where alkyne C-H and $\text{C}\equiv\text{C}$ stretches at 3296 and 2126 cm^{-1} in spectrum (b) disappeared after click reaction with AZT. Meanwhile, the peaks of 3158 cm^{-1} assigned to N-H of AZT (spectrum a) appeared in spectrum c, confirming that AZT has been successfully immobilized on the surface of the poly (PMA-co-PETA) monolithic skeleton via click reaction. (Fig.S2, Supporting information).

3.2. Effect of AZT content on chromatographic selectivity and retention behavior of poly (AZT-co-PMA-co-PETA) monolithic column.

In order to evaluate and compare the chromatographic properties of the poly (AZT-co-PMA-co-PETA) monoliths with different content of AZT, toluene, thiourea, formamide and N,N-dimethylformamide (DMF) were selected as test compounds and a mobile phase containing water/ACN was used. The solvent (MeOH) was selected as the void time marker in this system. The effect of ACN content in the mobile phase on the k values of the four test compounds with column A-D (Table 1) was shown in Fig.3. Taking column C as an example, it was seen that the neutral toluene showed a strong retention in the low ACN content and eluted after polar thiourea ranged from 30% to 65% (v/v %). Furthermore, the k value of toluene markedly decreased with increasing ACN content from 30% to 80% and was close to zero at the content of ACN over 80%, demonstrating a typical reversed-phase retention mechanism existed in the column C. Contrarily, thiourea showed no retention as the ACN content was in range of 30-70%. However, increasing k of thiourea could be obtained with the increase of ACN content from 70% to 100%. These results suggested a hydrophilic interaction chromatography (HILIC) retention mechanism at high ACN content (>70%). Similar results were also obtained while using column A, column B and column D as separation media. By comparison of Fig.3(a-d), however, it was clearly observed that the k value of thiourea

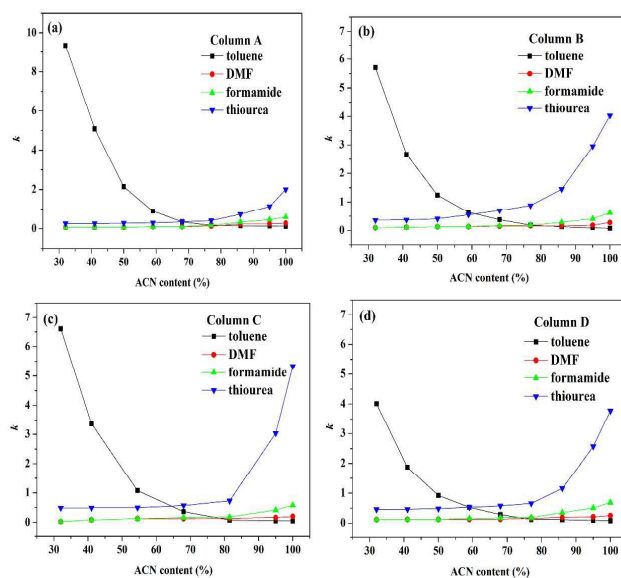


Fig.3. (a-d) Relationship between k and ACN concentration on the poly (AZT-co-PMA-co-PETA) monolithic column (column A, column B, column C and column D).

85 Conditions: (a-d): ACN/water; Flow rate (actual flow rate after splitting): 0.02 mL/min (80 nL/min); Detection wavelength: 214 nm; the analytes are (1) toluene (100 ppm); (2) DMF (100 ppm); (3) formamide (100 ppm); (4) thiourea (100 ppm).

in column C was 5.34 at 100% ACN, much higher than those obtained on column A, column B and column D under the same chromatographic condition. The results suggested that column C had a better hydrophilic interaction than column A, column B and column D. Therefore, the column C with the molar ratio of AZT to PMA with 1:1 and the mass ratio of AZT and PMA to PETA with 18:12 was used for further evaluation.

Presented in Fig.4(a) was the separation of the four solutes with the poly (AZT-co-PMA-co-PETA), poly (PMA-co-PETA), and AZT-modified poly (PMA-co-PETA) monoliths, respectively. It was observed that absolute baseline separation of toluene, DMF, formamide and thiourea could be achieved with the poly (AZT-co-PMA-co-PETA) monolith when a mobile phase of 100% ACN was adopted. The four solutes were eluted out in order of toluene < DMF < formamide < thiourea according to their polarity from low to high, suggesting a typical hydrophilic interaction liquid chromatography (HILIC) retention mechanism. However, the four test compounds were not well separated in the poly (PMA-co-PETA) monolith, which demonstrated that the introduction of AZT changed the surface of the poly ((PMA-co-PETA) monolith from mainly hydrophobic to hydrophilic. Compared with the boronic acid-based polymer monolith,³⁸ the as-prepared poly (AZT-co-PMA-co-PETA) showed good resolution and high separation ability. It should be noted that poor resolutions of the four solutes were observed in the AZT-modified poly (PMA-co-PETA) monolith while using the same mobile phase. More detailed evaluation and comparison on the resolution and column efficiency of the three polymer monoliths were listed in Table S1 (Supporting information). The results demonstrated that the synthesis method based on “one-pot” process is more efficient than the post modification.

The column efficiency of the poly (AZT-co-PMA-co-PETA) monolith was evaluated by changing the flow rate of the mobile phase in cLC. Fig.4(b) showed the relationship between the flow rate and the plate height for the four test solutes, in which the lowest plate height of ~21.1 μm was obtained with a flow velocity of 0.17 mm/s. Although high flow velocity favored the rapid separation, poor resolution and efficiency was obtained. In this case, a column efficiency varying from 35,000 to 48,000 plate/m was achieved for the three former solutes (toluene, DMF, and formamide) at the flow velocity of 0.17 mm/s. The run-to-run repeatability was assessed on a single capillary monolithic column, and the relative standard deviations (RSDs) for the k values of the four solutes were less than 0.8% ($n=5$). Both column-to-column and batch-to-batch repeatability for the preparation of monolithic columns were also evaluated, which were less than 2.6% ($n=3$) and 4.2% ($n=3$), respectively. These results demonstrated that the prepared poly (AZT-co-PMA-co-PETA) monoliths had good reproducibility. In addition, the life time of the prepared polymer monoliths was also examined and the result showed consecutive runs more than two months could be anticipated according to the present experiments, suggesting good stability of the prepared polymer monolith.

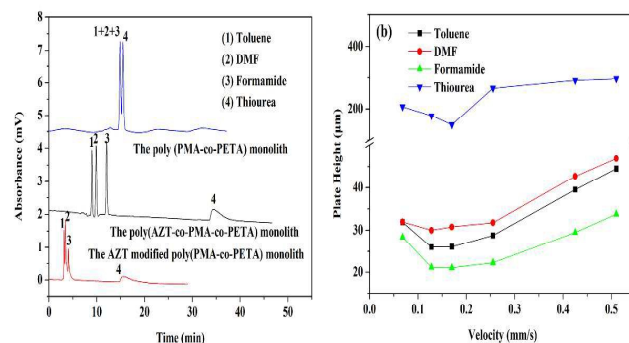


Fig.4. (a) Separation of four solutes with the poly (PMA-co-PETA), poly (AZT-co-PMA-co-PETA) and AZT-modified poly (PMA-co-PETA) monoliths; (b) Dependence of the plate height of four solutes on the linear velocity of the mobile phase by the poly (AZT-co-PMA-co-PETA) monolith (column C). Conditions: 100%ACN; Flow rate (actual flow rate after splitting): 0.02 mL/min (80 nL/min); Pump pressure: 2.2 MPa; Detection wavelength: 214 nm; the analytes are (1) toluene (100 ppm); (2) DMF (100 ppm); (3) formamide (100 ppm); (4) thiourea (100 ppm).

3.3. Reversed-phase chromatography of the poly (AZT-co-PMA-co-PETA) monolithic column.

As mentioned above, the poly (AZT-co-PMA-co-PETA) monolith can provide hydrophobic interaction at low ACN content and the separation ability of the monolith was tested by separating alkylbenzene analogues. A typical chromatogram was shown in Fig.5(a), which presented the baseline separation of five alkylbenzenes with the mobile phase of 45.5% (v/v) ACN/H₂O. The column efficiencies varying from 35000 to 62000 plates/m were achieved for the five alkylbenzenes. Furthermore, alkylbenzenes were eluted out in order of benzene < toluene < ethylbenzene < n-propylbenzene < naphthalene according to their hydrophobicity, confirming a typical reversed-phase separation mechanism. In addition, the effect of ACN content on the retention of the five alkylbenzenes was studied (Fig.5(b)), and the result showed that the $\log k$ values of the five alkylbenzenes decreased with the increase of ACN content, confirming again that the reversed-phase mechanism played a dominant role in the separation of the alkylbenzenes on the poly (AZT-co-PMA-co-PETA) monolith (The solvent (MeOH) was selected as the void time marker).

3.4. Hydrophilic interaction chromatography of the poly (AZT-co-PMA-co-PETA) monolithic column

As expected, the introduction of AZT on the surface of poly (AZT-co-PMA-co-PETA) monolith could be applied to the separation of amides in HILIC mode. It was observed from Fig.6(a) that the baseline separation of four amides was achieved on the poly (AZT-co-PMA-co-PETA) monolith. In comparison with the zwitterionic polymer monolith reported by Lee,³⁹ the poly (AZT-co-PMA-co-PETA) monolith showed high resolution and good peak shape. Accordingly, the column efficiencies of DMF, N,N-dimethylacetamide, formamide and N,N'-methylene bisacrylamide were 50000, 58000, 31000, and 20000 plates/m, respectively. The retention order in the poly (AZT-co-PMA-co-PETA) monolith was DMF < N,N-dimethylacetamide < formamide < N,N'-methylene bisacrylamide. (The retention time of toluene was selected as t_0 value) Besides, the corresponding k values increased with the increase of ACN content (Fig.6(b)). Obviously, the HILIC mechanism originated from AZT can respond to the separation of the four amides based on the above results.

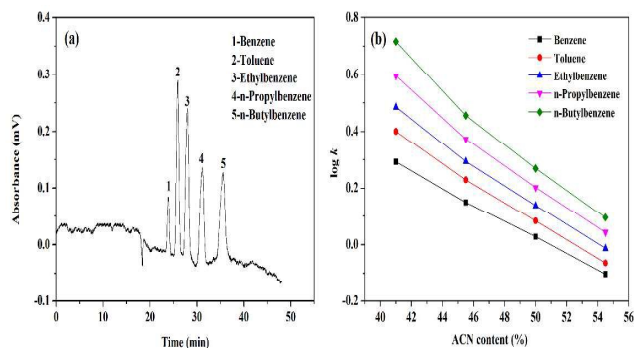


Fig.5.(a) Hydrophobic interaction chromatography for the separation of alkylbenzenes and (b) effect of ACN content on the k values of alkylbenzenes on the poly (AZT-co-PMA-co-PETA) monolith (column C).

Conditions for (a): Mobile phase: ACN/water: 45.5/54.5 (v/v %); Flow rate (actual flow rate after splitting): 0.02 mL/min (80 nL/min); Pump pressure: 4.8 MPa; Detection wavelength: 214 nm; For (b), all the conditions are same as (a) except for ACN content; (a) the analytes are (1) benzene (100 ppm); (2) toluene (100 ppm); (3) ethylbenzene (100 ppm); (4) n-propylbenzene (100 ppm); (5) n-butylbenzene (100 ppm).

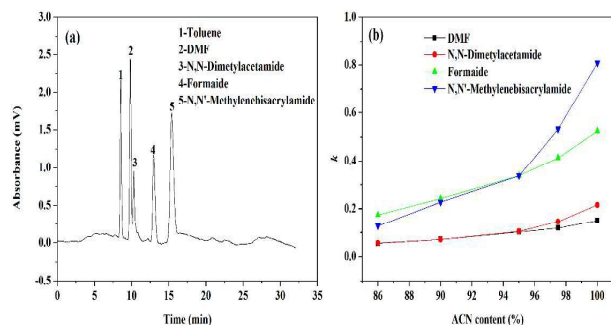


Fig.6. (a) Hydrophilic interaction chromatography for the separation of amides and (b) effect of ACN content on the k values of amides on the poly (AZT-co-PMA-co-PETA) monolith (column C).

Conditions for (a): Mobile phase: 100%ACN; Flow rate (actual flow rate after splitting): 0.02 mL/min (80 nL/min); Pump pressure: 2.2 MPa; Detection wavelength: 214 nm; For (b), all the conditions are same as (a) except for ACN content; (a) the analytes are (1) toluene (100 ppm); (2) DMF (100 ppm); (3) N,N-dimethylacetamide (100 ppm); (4) formamide (100 ppm); (5) N,N'-methylene bisacrylamide (100 ppm).

3.5. Cation-exchange/hydrophobic interaction chromatography of the poly (AZT-co-PMA-co-PETA) monolithic column

The poly (AZT-co-PMA-co-PETA) monolith can offer electrostatic interaction with charged analytes due to the existence of multiple ionizable moieties (pK_{a1} -3.0 (N), and pK_{a2} 9.96 (NH)) on the monolithic surface. To demonstrate the selectivity of the poly (AZT-co-PMA-co-PETA) monolith to charged analytes, four anilines (phenylamine (pK_a 4.6), o-nitroaniline (pK_a -0.28), *a*-naphthylamine (pK_a 3.92), and o-phenylenediamine (pK_a 4.52)) were used for the evaluation. As shown in Fig.7(a), an absolute baseline separation of the four anilines was obtained with 50% ACN in 150 mM PB at pH 7.0. At pH 7.0, all analytes were deprotonated, and thus the electrostatic interaction between the analytes and the polymer monolith was weak. When the pH of the mobile phase decreased to 4.0, phenylamine and o-phenylenediamine was protonated, which may have significant electrostatic interaction with the negatively charged monolithic surface to cause strong retention on the poly (AZT-co-PMA-co-PETA) monolith. The electrostatic interaction between anilines except o-nitroaniline with the monolithic surface was much stronger so that the three anilines could not be eluted within 60 min when the pH of mobile phase

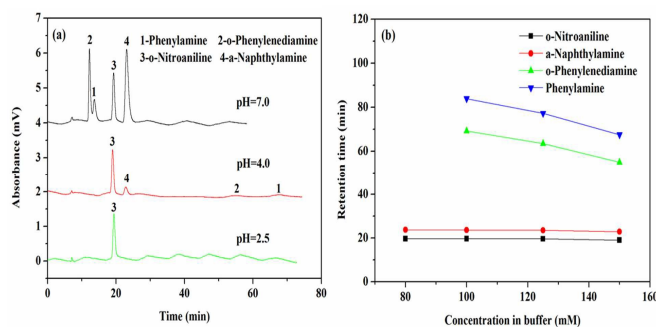


Fig.7. (a) Cation-exchange/hydrophobic interaction chromatography for the separation of anilines at varying pH and (b) effect of salt concentration on retention time of anilines on the poly (AZT-co-PMA-co-PETA) monolith (column C).

Conditions for (a): Mobile phase: 150 mM PB containing 50% (v/v) ACN with various pH; Pump pressure: 4.6 MPa; Flow rate (actual flow rate after splitting): 0.02 mL/min (80 nL/min); Detection wavelength: 214 nm; For (b), all the conditions are same as (a) except for pH 4.0; the analytes are (1) phenylamine (100 ppm); (2) o-phenylenediamine (100 ppm); (3) o-nitroaniline (100 ppm); (4) *a*-naphthylamine (100 ppm).

was 2.5. The results were attributed to the strong electrostatic interaction between anilines and the poly (AZT-co-PMA-co-PETA) monolith.

Additionally, the effect of salt concentration on the retention of the four anilines was investigated by varying the concentration of PB (pH 4.0) from 80 to 150 mM in the mobile phase of ACN/water (50/50,v/v), which was shown in Fig.7(b). As the concentration of PB increased, the ion-exchange interaction between the anilines (phenylamine and o-phenylenediamine) and the stationary phase weakened, which resulted in decreasing retention times. However, the retention time of the other two anilines almost kept constant. The above results demonstrated that the cation-exchange interaction played a dominant role in the separation of the four anilines.

The content of ACN in the mobile phase had significant influence on the separation of the four anilines. As shown in Fig.S3 (Supporting information), the retention times of the four anilines decreased with the increase of ACN content from 41 to 54.5%. The results suggested that the separation of these anilines was mainly based on hydrophobic interaction between the analytes and the monolithic stationary phase. Overall, the separation of four anilines was based on two combined effect of cation-exchange interaction and hydrophobic interaction in low content of ACN at pH 4.0.

The separation of benzoic acids was further demonstrated that AZT offered negative charge. Fig.S4(a) (Supporting information) showed the separation of four benzoic acids, including salicylic acid (pK_a 2.81), *p*-hydroxybenzoic acid (pK_a 4.58), 2,4-dihydroxybenzoic acid (pK_a 3.29) and isophthalic acid (pK_a 3.50) in the mobile phase of ACN/PB with various pH. In comparison of their retention time and elution order, it can be concluded that the electrostatic repulsion between benzoic acids and the monolithic stationary phase was existed. The retention factors of four benzoic acids decreased with the increase of ACN content from 36.5 to 50%, which suggested that the hydrophobic interaction played a major role in the separation of four benzoic acids (Fig.S4(b), Supporting information). The effect of salt concentration on the retention of benzoic acids was investigated by varying the concentration of PB (pH4.0) from 20 to 100 mM in the mobile phase of ACN/water (36.5/63.5,v/v %), which was shown in Fig.S4(c)(Supporting information). The results demonstrated that the electrostatic repulsion existed.

3.6. Cation-exchange/hydrophilic interaction chromatography of the poly (AZT-co-PMA-co-PETA) monolithic column

A hydrophilic partitioning/cation exchange interaction was also evaluated by the separation of five benzoic acids (benzoic acid (pKa 4.20), salicylic acid (pKa 2.81), p-hydroxybenzoic acid (pKa 4.58), 2,4-dihydroxy benzoic acid (pKa 3.29) and isophthalic acid (pKa 3.50)). Fig. 8(a) showed a good separation of benzoic acids on the poly (AZT-co-PMA-co-PETA) monolith with the mobile phase of 20 mM PB containing 90.5% (v/v) ACN at various pH (The retention time of toluene was selected as t_0 value). It should be noted that varying the pH of mobile phase from 3.0 to 7.0 (keeping 90.5% ACN/20 mM PB constant) did not lead to the change in the elution order of the five benzoic acids, suggesting that no electrostatic interaction between benzoic acids and AZT occurred at high ACN content. In contrast, the k values of the five benzoic acids gradually increased with the increase of ACN content from 77% to 90.5%, which was in good agreement with the mechanism described for HILIC (Fig.8(b)).

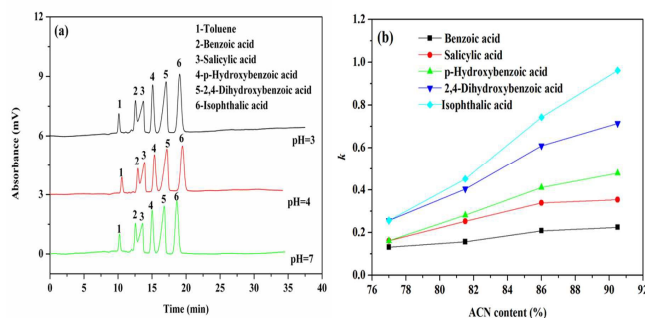


Fig.8. (a) Cation-exchange/hydrophilic interaction chromatography for the separation of benzoic acids at varying pH and (b) effect of ACN content on the k values of benzoic acids on the poly (AZT-co-PMA-co-PETA) monolith (column C).

Conditions for (a): Mobile phase: 20 mM PB containing 90.5% (v/v) ACN with various pH; Pump pressure: 2.4 MPa; Flow rate (actual flow rate after splitting): 0.02 mL/min (80 nL/min); Detection wavelength: 214 nm; For (b), all the conditions are same as (a) except for pH 4.0; the analytes are (1) toluene (100 ppm); (2) benzoic acid (100 ppm); (3) salicylic acid (100 ppm); (4) p-hydroxybenzoic acid (100 ppm); (5) 2,4-dihydroxy benzoic acid (100 ppm); (6) isophthalic acid (100 ppm).

3.7. Applications

3.7.1 Separation of sulfonamide antibiotics

Sulfonamide antibiotics, widely used in animal husbandry for the prevention or treatment of diseases and growth-promoting purposes, were used to evaluate the applicability of the poly (AZT-co-PMA-co-PETA) monolith. As can be seen from Fig.9(a), almost baseline separation of five sulfonamide antibiotics (sulfadiazine (SDZ, pK_{a1} =1.64, pK_{a2} =6.50), sulfamerazine (SMR, pK_{a1} =1.64, pK_{a2} =6.98), sulfamethazine (SMZ, pK_{a1} =1.95, pK_{a2} =7.45), sulfapyridine (SPD, pK_{a1} =2.90, pK_{a2} =8.54) and sulfisoxazole (SIZ, pK_{a1} =1.52, pK_{a2} =4.83), their chemical structures were shown in Fig.S5, Supporting information) on the poly (AZT-co-PMA-co-PETA) monolith was achieved within 12 min when using 32% ACN/PB (100 mM, pH 7.0). Compared to the poly (divinylbenzene-alkyl methacrylate) monolithic column reported by Cheng,⁴⁰ the proposed monolith in current work showed more short time to separate the sulfonamide antibiotics. It should be noted that their peak shape has a little tailing (the tailing factors of SIZ, SDZ, SMR, SMZ and SPD are 1.22, 1.08, 1.03, 1.06, 1.13, respectively), which was likely due to the presence of weak electrostatic attractions between the negatively charged monolithic surface and the sulphonamide cations. Additionally, the retention time of the five sulfonamide antibiotics decreased with increasing ACN contents from 32 to 45.5% in the mobile phase (Fig.9(b)), indicating that

the hydrophobic interaction played a dominant role in the separation of the five sulfonamide antibiotics.

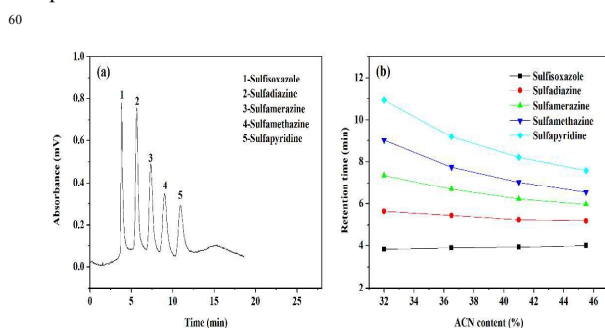


Fig.9. (a) Separation of sulfonamide antibiotics and (b) effect of ACN content on retention time of sulfonamide antibiotics on the poly (AZT-co-PMA-co-PETA) monolith (column C).

Conditions for (a): Mobile phase: 100 mM PB containing 32% (v/v) ACN at pH 7.0; Flow rate (actual flow rate after splitting): 0.035 mL/min (140 nL/min); Pump pressure: 7.2 MPa; Detection wavelength: 214 nm; For (b), all the conditions are same as (a) except for ACN content; (a) the analytes are (1) sulfisoxazole (100 ppm); (2) sulfadiazine (100 ppm); (3) sulfamerazine (100 ppm); (4) sulfamerazine (100 ppm); (5) sulfapyridine (100 ppm).

3.7.2 Separation of nucleosides, nucleobases and anesthetics

Separation of basic compounds is still a tough task in cLC with reversed-phase mode due to the multiplicity of their polar and positively charged groups. As an alternative, HILIC or HILIC/cation-exchange mode was preferred, Fig.10(a) showed the baseline separation of six anesthetics (the chemical structures of papaverine, triazolam, pemoline, codeine, morphine and adanon were shown in Fig.S6, Supporting information) was also obtained on the poly (AZT-co-PMA-co-PETA) monolith with the mobile phase of 20 mM PB containing 90.5% (v/v) ACN at pH 7.0 (The solvent of MeOH was selected as the void time marker). Moreover, the k values of the six anesthetics gradually increased with the increase of ACN content from 77% to 90.5%, which was in good agreement with the mechanism described as HILIC (Fig.10(b)). To demonstrate the feasibility of the poly (AZT-co-PMA-co-PETA) monolith for real-world sample, analysis of urine sample was performed. Compared to the urine blank (Fig.10(c)), four spiked nucleosides and nucleobases (their chemical structures were listed in Fig.S7, Supporting information) were well separated in the poly (AZT-co-PMA-co-PETA) monolith with the mobile phase of 20 mM PB containing 86% (v/v) ACN at pH 7.0, as shown in Fig.10(d). Moreover, the proposed poly (AZT-co-PMA-co-PETA) monolith showed good resolution and peak shape for nucleoside separation, compared with our previous work.³⁸ In addition, the k values of the four nucleosides and nucleobases gradually increased with the increase of ACN content from 77% to 90.5%, which was in good agreement with the mechanism described as HILIC. The results further confirmed that HILIC mode of the poly (AZT-co-PMA-co-PETA) monolith is a good alternative to the polar analytes.

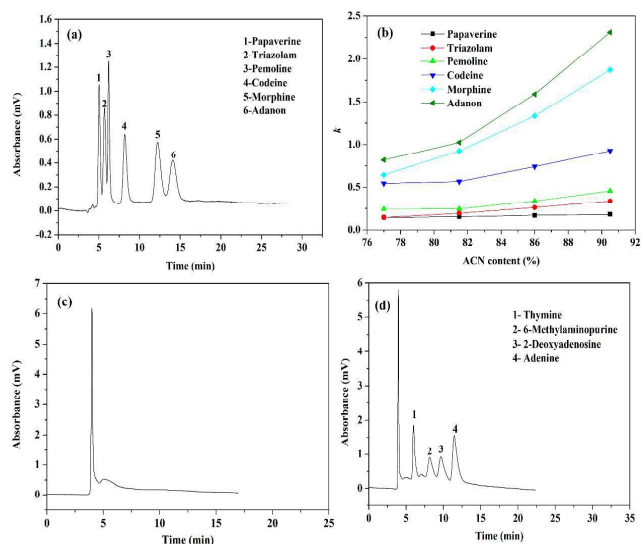


Fig.10. (a) Separation of anesthetics and (b) effect of ACN content on the k' values of anesthetics on the poly(AZT-co-PMA-co-PETA) monolith (column C). (c) Separation of blank urine and (d) urine spiked with four nucleosides on the poly (AZT-co-PMA-co-PETA) monolith (column C).

Conditions for (a): For (a), mobile phase: 20 mM PB containing 90.5% (v/v) ACN at pH 7.0; Flow rate(actual flow rate after splitting): 0.035 mL/min (140 nL/min); Pump pressure: 3.8 MPa; Detection wavelength: 214 nm; For (b), all the conditions are same as (a) except for ACN content; the analytes are (1) papaverine (100 ppm); (2) triazolam (100 ppm); (3) pemoline (100 ppm); (4) codeine (100 ppm); (5) morphine (100 ppm); (6) adanon (100 ppm). For (c), Mobile phases: 20 mM PB containing 86% (v/v) ACN at pH 7.0; Flow rate (actual flow rate after splitting): 0.035 mL/min (140 nL/min); Pump pressure: 4.2 MPa; Detection wavelength: 214 nm; For (d), all the conditions are same as (c), the analytes are (1) thymine (100 ppm); (2) 6-methylaminopurine (100 ppm); (3) 2-deoxyadenosine (100 ppm); (4) adenine (100 ppm).

3.7.3 Separation of proteins

As mentioned above, the produced poly (AZT-co-PMA-co-PETA) monolith exhibited adequate separation selectivity and efficiency, and then it is expected to be applied to the separation of complex analytes such as proteins. The applicability of the poly (AZT-co-PMA-co-PETA) monolith for macromolecule separation was evaluated by gradient elution of protein mixture including HRP, Cyt C, Mb, Hb and Trf. As presented in Fig.11, five proteins were well separated within 20 min based on reversed-phase mode by using a simple gradient elution with ACN in 0.1% (v/v) trifluoroacetic acid (TFA) aqueous solution at a linear velocity of 0.297 mm/s. Although better peak shape of proteins can be obtained by further optimizing gradient elution, resolutions of proteins would deteriorate. Therefore, the above gradient elution was adopted as a compromise. All the above results confirmed that the produced poly (AZT-co-PMA-co-PETA) monolith allowed efficient separations of a large variety of compounds, ranging from small organic compounds to large biological molecules.

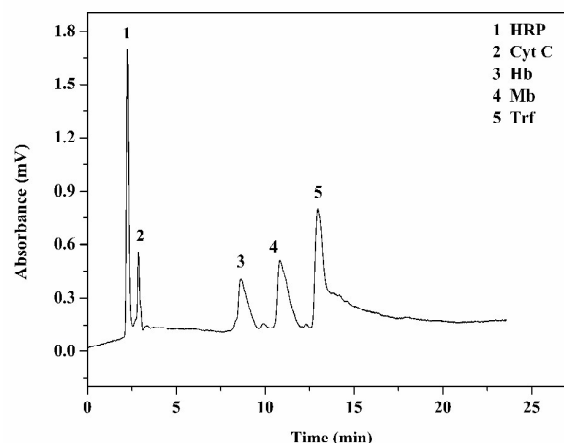


Fig.11. Separation of five proteins on the poly (AZT-co-PMA-co-PETA) monolith (column C).

Conditions: Mobile phase: (A) 5% ACN + 0.1%(v/v) TFA; (B) 95% ACN; Linear gradient: from 20% B to 50% B within 0–40 min; Flow rate(actual flow rate after splitting): 0.035 mL/min (140 nL/min); Pump pressure: 6.0–7.8MPa; Detection wavelength: 214 nm; the analytes are (1) HRP (100 ppm); (2) Cyt C (100 ppm); (3) Hb(100 ppm); (4) Mb (100 ppm); (5) Trf (100 ppm).

4. Conclusion

In summary, a facile method was developed for preparation of the polymer monoliths by the combination of the free radical polymerization and CuAAC click reaction in one pot. The synthesis method was simple, efficient and time-saving, compared to the conventional post click modification. Comprehensive investigation of the poly (AZT-co-PMA-co-PETA) monolith confirmed that the polymer monolith had the excellent chromatographic performances in terms of hydrophobicity, hydrophilicity and cation-exchange interaction. The successful separation of a series of small molecules and proteins also indicated the solid potential of this strategy for the preparation of the polymer monoliths with the desirable functional monomers.

Acknowledgements

We gratefully acknowledge the financial support from the National Natural Science Foundation of China (21375018 and 21175025), and the Natural Science Foundation of Fujian Province (2014J01402).

References

- 1 F. Svec and J.M.J. Fréchet, *Science*, 1996, **273**, 205-211.
- 2 L.B. Ren, Z. Liu, Y.C. Liu, P. Dou and H.Y. Chen, *Angew. Chem. Int. Ed*, 2009, **48**, 6704-6707.
- 3 M.H. Wu, R.A. Wu, F.J. Wang, L.B. Ren, J. Dong, Z. Liu and H.F. Zou, *Anal. Chem*, 2009, **81**, 3529-3536.
- 4 Y. Wen and Y.Q. Feng, *J. Chromatogr. A*, 2007, **1160**, 90-98.
- 5 J. Krenkova, N.A. Lacher and F. Svec, *Anal. Chem*, 2009, **81**, 2004-2012.
- 6 R. Mallik, T. Jiang and D.S. Hage, *Anal. Chem*, 2004, **76**, 7013-7022.
- 7 V. Frankovič, A. Podgornik, N.L. Krajnc, F. Smrekar, P. Krajnc and A. Štrancar, *J. Chromatogr. A*, 2008, **1207**, 84-93.
- 8 H.C. Kolb, M.G. Finn and K.B. Sharpless, *Angew. Chem. Int. Ed*, 2001, **40**, 2004-2021.
- 9 P.L. Golas and K. Matyjaszewski, *Chem. Soc. Rev*, 2010, **39**, 1338-1354.
- 10 R. Manova, T.A.V. Beek and H. Zuilhof, *Angew. Chem. Int. Ed*, 2011, **50**, 5428-5430.

- 11 D. Zhao, S.W. Tan, D.Q. Yuan, W.G. Lu, Y.H. Rezenom, H.L. Jiang, L.Q. Wang and H.C. Zhou, *Adv. Mater*, 2011, **23**, 90-93. 70
- 12 J.F. Lutz and Z. Zarafshani, *Advanced Drug Delivery Reviews*, 2008, **60**, 958-970. 5
- 13 Y.Z. Chen, M.H. Wu, K.Y. Wang, B. Chen, S.Z. Yao, H.F. Zou and L.H. Nie, *J. Chromatogr. A*, 2011, **1218**, 7982-7988.
- 14 Y.Z. Chen, K.Y. Wang, H.H. Yang, Y.X. Liu, S.Z. Yao, B. Chen, L.H. Nie and G.M. Xu, *J. Chromatogr. A*, 2012, **1233**, 91-99. 75
- 15 Z.A. Lin, X.Q. Tan, R.F. Yu, J.S. Lin, X.F. Yin, J.Wang, L. Zhang, and H.H. Yang, *J. Chromatogr. A*, 2014, **1355**, 228-237.
- 16 W.G. Lewis, L.G. Green, F. Grynszpan, Z. Radić, P.R. Carlier, P. Taylor, M.G. Finn and K.B. Sharpless, *Angew. Chem. Int. Ed*, 2002, **41**, 1053-1057. 80
- 17 V. Ladmiral, G. Mantovani, G.J. Clarkson, S. Cauet, J.L. Irwin and D.M. Haddleton, *J. Am. Chem. Soc*, 2006, **128**, 4823-4830. 85
- 18 C.H. Chu and R.H. Liu, *Chem. Soc. Rev*, 2011, **40**, 2177-2188.
- 19 K. Zhu, Y. Zhang, S. He, W.W. Chen, J.Z. Shen, Z. Wang and X.Y. Jiang, *Anal. Chem*, 2012, **84**, 4267-4270.
- 20 M.A. Quadir, M. Martin, P.T. Hammond, *Chem. Mater*, 2014, **26(1)**, 461-476. 90
- 21 Y.P. Zhang, Z.M. Guo, J.X. Ye, Q. Xu, X.M. Liang and A.W. Lei, *J. Chromatogr. A*, 2008, **1191**, 188-192.
- 22 Z.M. Guo, A.W. Lei, Y.P. Zhang, Q. Xu, X.Y. Xue, F.F. Zhang and X.M. Liang, *Chem. Commun*, 2007, 2491-2493.
- 23 H.Y. Guo, R.H. Liu, J.J. Yang, B.C. Yang, X.M. Liang and C.H. Chu, *J. Chromatogr. A*, 2012, **1223**, 47-52. 95
- 24 M.Y. Xue, H.X. Huang, Y.X. Ke, C.H. Chu, Y. Jin and X.M. Liang, *J. Chromatogr. A*, 2009, **1216**, 8623-8629.
- 25 M. Slater, M. Snauko, F. Svec and J.M.J. Fréchet, *Anal. Chem*, 2006, **78**, 4969-4975. 100
- 26 M. Guerrouache, M.C. Millot and B. Carbonnier, *Rapid Commun*, 2009, **30**, 109-113.
- 27 J.L. Guo, Q.X. Zhang, Y.B. Peng, Z.H. Liu, L.Y. Rao, T. He, J. Crommen, P.H. Sun and Z.J. Jiang, *J. Sep. Sci*, 2013, **36**, 2441-2449. 105
- 28 X.L. Sun, D. Lin, X.W. He, L.X. Chen and Y.K. Zhang, *Talanta*, 2010, **82**, 404-408.
- 29 X.L. Sun, X.W. He, L.X. Chen and Y.K. Zhang, *Anal. Biochem*, 2011, **399**, 3407-3413.
- 30 M.H. Wu, H.Q. Zhang, Z.X. Wang, S.W. Shen, X.C. Le and X.F. Li, *Chem. Commun*, 2013, **49**, 1407-1409. 110
- 31 H. Mitsuya, K.J. Weinhold, P.A. Furman, M.H.S. Clair, S.N. Lehrman, R.C. Gallo, D. Bolognesi, D.W. Barry and S. Broder, *Proc. Natl. Acad. Sci. USA*, 1985, **82**, 7096-7100.
- 32 R. Yarchoan, H. Mitsuya, C.E. Myers and S. Broder, *N. Engl. J. Med*, 1989, **321**, 726-738. 115
- 33 L.B. Ren, Z. Liu, M.M. Dong, M.L. Ye, H.F. Zou, *J. Chromatogr. A* 2009, **1216**, 4768-4774.
- 34 T. Hara, S. Makino, Y. Watanabe, T. Ikegami, K. Cabrera, B. Smarsly and N. Tanaka, *J. Chromatogr. A*, 2010, **1217**, 89-98. 120
- 35 P.S. Nikam, L.N. Shirsat and M. Hasan, *J. Chem. Eng. Data*, 1998, **43**, 732-737.
- 36 Y. Li, B.H. Gu, H.D. Tolley and M.L. Lee, *J. Chromatogr. A*, 2009, **1216**, 5525-5532.
- 37 Q.X. Zhang, J.L. Guo, F. Wang, J. Crommen and Z.J. Jiang, *J. Chromatogr. A*, 2014, **1325**, 147-154. 125
- 38 H. Huang, Z.A. Lin, Y. Lin, X.B. Sun, Y.Y. Xie, L. Zhang and G.N. Chen, *J. Chromatogr. A*, 2012, **1251**, 82-90.
- 39 X. Chen, H.D. Tolley, M.L. Lee, *J. Sep. Sci*, 2011, **34**, 2088-2096. 130
- 40 Y.J. Cheng, S.H. Huang, B. Singco and H.Y. Huang, *J. Chromatogr. A*, 2011, **1218**, 7640-7647.

1
2
3
4
5
6 5
7
8
9
10 10
11
12
13
14
15 15
16
17
18
19 20
20
21
22
23 25
24
25
26
27
28
29
30
31
32
33
34
35
36
37
38
39
40
41
42
43
44
45
46
47
48
49
50
51
52
53
54
55
56
57
58
59
60